Inelastic Collisions of a Fermi Gas in the BEC-BCS Crossover

X. Du, Y. Zhang, and J. E. Thomas*
Duke University, Department of Physics, Durham, North Carolina, 27708, USA
(Dated: March 10, 2009)

We report the measurement of inelastic three-body and two-body collisional decay rates for a two-component Fermi gas of ^{6}Li, which are highly suppressed by the Pauli exclusion principle. Our measurements are made in the BEC-BCS crossover regime, near the two-body collisional (Feshbach) resonance. At high temperature (energy) the data shows a dominant three-body decay process, which is studied as a function of bias magnetic field. At low energy, the data shows a coexistence of two-body and three-body decay processes near and below the Feshbach resonance. Below resonance, the observed two-body inelastic decay can arise from molecule-atom and molecule-molecule collisions. We suggest that at and above resonance, an effective two-body decay rate arises from collisions between atoms and correlated (Cooper) pairs that can exist at sufficiently low temperature.

Quantum statistics dramatically affects the inelastic collision rates that determine the lifetime of cold atomic gases. In an inelastic three-body collision, two of the colliding atoms decay to a bound molecular state, releasing energy. Interactions between atoms can be strongly enhanced by tuning a bias magnetic field near a collisional (Feshbach) resonance [1, 2]. In a Bose gas, this enhancement is accompanied by an inelastic collision rate that increases by two or three orders of magnitude compared to that obtained away from resonance [3], and a correspondingly short lifetime of just a few ms at typical atomic densities. In contrast, for a Fermi gas in a mixture of one or two different spin states, the probability of three atoms colliding is highly suppressed by the Pauli exclusion principle. The lifetime of the cloud is on the order of 0.1 s for fermionic ^{40}K [4, 5] and 50 s for ^{6}Li [6, 7]. The long lifetime of Fermi gases is essential to the study of strongly interacting Fermi gases [8, 9], which offers unprecedented opportunities to test nonperturbative theoretical techniques that apply to exotic systems ranging from high temperature superconductors to nuclear matter. Determination of the inelastic collision rate coefficients in the strongly interacting regime of a Fermi gas provides new tests of few-body theories [10, 11, 12, 13, 14, 15, 16, 17, 18].

In this Letter we report on the precision measurement of three-body inelastic collision rate constants K_3 for an ultracold two-component Fermi gas in the BEC-BCS crossover regime near a Feshbach resonance. We also observe two-body inelastic decay below the Feshbach resonance, which arises from molecules [7, 16]. From the data, we estimate the corresponding rate constants K_2. Finally, we observe two-body decay at and just above the Feshbach resonance. We suggest that this process arises from correlated pairs, which is a many-body effect. We load a Fermi gas from a single beam CO_2 laser trap into a CO_2 laser standing wave that is formed by the incoming and retro-reflected beam. The standing wave produces a potential with a period of 5.3 μm that is four times deeper than that of the single beam trap and tightly confining in the axial direction (along the standing wave). The corresponding atomic density is up to $10^{14}/\mathrm{cm}^3$, ~ 20 times higher than that obtained in the single optical trap. This dramatically increases the inelastic collision rates, making precise measurement of the rate constants feasible.

For two-component Fermi gases, three-body inelastic collisions arise in the BEC-BCS crossover for processes of the form $F+F+F' \rightarrow F+(FF')$, where F and F' are fermions in different states and (FF') is a bound molecular state. On the BEC side of the Feshbach resonance where the scattering length $a > 0$, the three-body decay rate is predicted to scale as a^6 [13, 15], while on the BCS side ($a < 0$), it should scale as $|a|^{2.455}$ [13]. By contrast, two-body inelastic collisions can arise from the decay of real molecules, which exist on the BEC side. These processes take the form either $(FF') + F \rightarrow (FF')_- + F$ or $(FF') + (FF') \rightarrow (FF')_- + (FF')$, where $(FF')_-$ is a deeply bound molecular state. The theory predicts that the decay rate scales as $a^{-3.33}$ for atom-molecule collisions or $a^{-2.55}$ for molecule-molecule collisions [16].

In the experiments, a sample of ^{6}Li atoms in a 50-50 mixture of the two lowest hyperfine states is loaded into a CO_2 laser trap with a bias magnetic field of 840 G, where the two states are strongly interacting. Evaporative cooling is performed to lower the temperature of the sample [8]. The magnetic field is then changed in 0.8 seconds to a final magnetic field where we perform the measurement. Subsequently, the gas is adiabatically loaded into a CO_2 laser standing wave by slowly turning on the retro-reflected CO_2 laser beam. A quasi-two-dimensional Fermi gas is then formed and absorption images are taken at various times after the formation of the 2-D system to determine the inelastic decay rate.

At the final optical trap depth, the measured trap oscillation frequencies in the standing wave are $\omega_\perp = 2\pi \times 3250$ Hz in the transverse directions and $\omega_z = 2\pi \times 83.5$ kHz in the axial direction. The corresponding frequencies in the single beam trap are $\omega_\perp = 2\pi \times 1650$ Hz and $\omega_z = 2\pi \times 56$ Hz, respectively. Our measurements indicate very good standing wave alignment, as the transverse frequency is nearly twice that of the single beam trap, as expected.

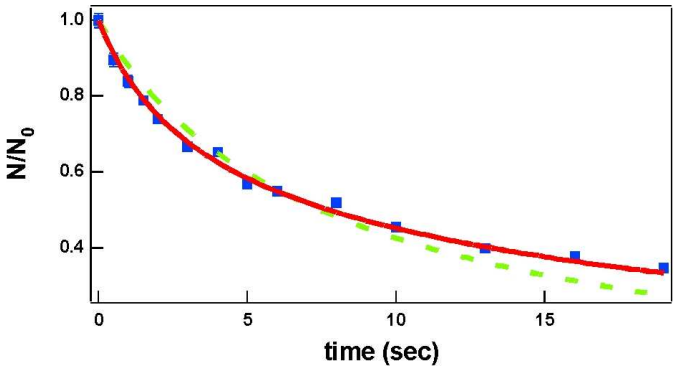

FIG. 1: Atom number versus time. Data were taken at 834 G and $E_\perp/E_{F\perp} = 1.8$. N is total atom number and N_0 is initial atom number in the observed region of the cloud. Blue dots: Experimental data; Red solid curve: Three-body decay fit; Green dashed line: Two-body decay fit.

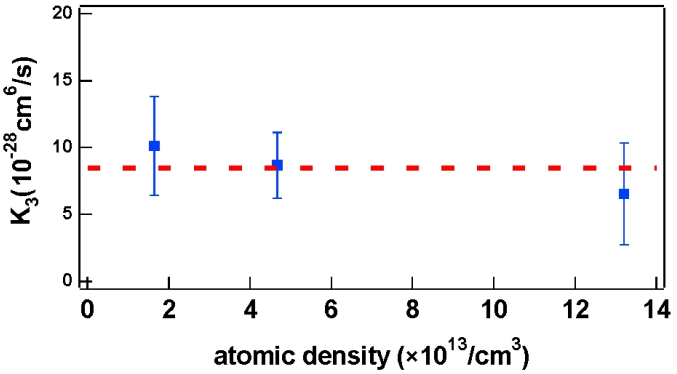

FIG. 2: Three-body inelastic collision rate coefficient K_3 versus atomic density for $E_\perp/E_{F\perp} = 1.8$. Blue dots: Experimental data. Error bars indicate statistical errors; Red dashed line: Fit to the data with $K_3 = (8.44 \pm 1.04) \times 10^{-28}\mathrm{cm}^6/\mathrm{s}$.

The total energy of the gas obeys the virial theorem [19] when the bias magnetic field is tuned to a broad Feshbach resonance, where the Fermi gas is unitary. Since the trap depth is large compared to the energy of the cloud, the confining potential U is approximately harmonic. Then the total energy is $E = 2\langle U\rangle = E_z + E_\perp$, where E_z is the axial energy and $E_\perp$ is the transverse energy, referred to the trap minimum. We determine only the transverse energy $E_\perp = 2m\omega_\perp^2\langle x^2\rangle$, by measuring the mean square transverse cloud size $\langle x^2\rangle$. For reference, the transverse energy for the ground state of an ideal two dimensional Fermi gas is $E_{I\perp} = \frac{2}{3}E_{F\perp}$, where $E_{F\perp}$ is the transverse Fermi energy, $E_{F\perp} = \hbar\omega_\perp N_s^{1/2}$. Here m is atomic mass of ^{6}Li and N_s is the total atom number in one site. For our experiments in the unitary gas, we measure $E_\perp/E_{F\perp} \sim 1.8$ with $N_s = 2,600$ and $E_\perp/E_{F\perp} \sim 0.7$ with $N_s = 1,600$. If the 2D unitary gas has the same effective mass as the 3D case, the 2D ground state transverse energy would be $2E_{F\perp}\sqrt{1+\beta}/3 \simeq 0.42\,E_{F\perp}$, using $\beta = -0.60$ [20]. In this case, our lowest energy would be significantly above the ground state value.

In general, for magnetic fields away from resonance where the scattering length is finite, the total energy is dependent on the scattering length [21]. In this case, we measure the number-independent mean square transverse cloud size $\langle x^2\rangle/x_{F\perp}^2$, where $x_{F\perp}^2$ is defined by $2m\omega_\perp^2 x_{F\perp}^2 \equiv E_{F\perp}$. For an ideal gas in the ground state, we note that $\langle x_0^2\rangle = \frac{2}{3}x_{F\perp}^2$.

We measure inelastic collision rates by measuring the time dependence of the atom number and the radial cloud size. The atom number N as a function of time is [3]

$$\frac{dN}{dt} = -\Gamma N - \int K_2\, n^2\, d^3x - \int K_3\, n^3\, d^3x, \qquad (1)$$

where n is the atomic density. On the right side, the first term arises from background collisions with a density-independent rate Γ ($1/\Gamma = 64$ s for our trap). The second term arises from loss due to two-body inelastic collisions with a rate coefficient K_2, while the third term arises from loss due to three-body collisions with a rate coefficient K_3.

For the conditions of our experiments, where $E_{F\perp}/\hbar\omega_z \simeq 1.5$, the ground axial state contains 90% of the atoms for an ideal Fermi ga at zero temperature. For simplicity, assume that the 2-D Fermi gas is primarily in the ground axial state of a single site. Then, the atomic density is

$$n(\rho, z) = \frac{2}{\pi^{3/2}}\frac{N(z)}{\sigma_\perp^2\sigma_z}\left(1 - \frac{\rho^2}{\sigma_\perp^2}\right)\exp\left(-\frac{z^2}{\sigma_z^2}\right), \qquad (2)$$

for $0 \le \rho \le \sigma_\perp$. Here, $N(z)$ is atom number in the site at position z. $\sigma_\perp$ is transverse width for a fit of a Thomas-Fermi distribution to the atomic density profile in the transverse directions, $\sigma_z = (\frac{\hbar}{m\omega_z})^{1/2}$ is axial width for the ground state (along the standing wave), and ω_z is the corresponding axial trap frequency.

In our experiments, $N(z)$ varies as a gaussian distribution function of z with width L_z over the whole cloud in the axial direction. Strictly speaking, $\sigma_\perp$, σ_z and ω_z also vary with z since the depth $U(z)$ of the potential for a site at z is a Lorentzian function of z. However, we measure a restricted part of the cloud from $z = -0.83\,L_z$ to $z = 0.83\,L_z$ over which $U(z)$ varies less than 10%. Hence, to good approximation, $\sigma_\perp$, σ_z and ω_z are spatially constant.

Integrating the atomic density over each well and then over the restricted region of the cloud, we obtain from Eq. 1

$$\frac{dN_c}{dt} = -\Gamma N_c - \alpha_2 K_2 \frac{N_c^2}{\sigma_\perp^2(t)\sigma_z} - \alpha_3 K_3 \frac{N_c^3}{\sigma_\perp^4(t)\sigma_z^2}, \qquad (3)$$

where N_c is total number of atoms in the restricted region. Here $\alpha_2 = \frac{2\sqrt{2}}{3}\pi^{-3/2}$ and $\alpha_3 = \frac{2}{\sqrt{3}}\pi^{-3}$. Note that $\sigma_\perp(t)$ is a function of time since heating leads to an increase in temperature and hence the width of the cloud

during the atom loss process. Typically $\sigma_\perp^2(t)$ and $\sigma_\perp^4(t)$ can be fit well to exponential curves, $\propto \exp(\gamma t)$. Note that at the highest energies used in our experiments, a significant fraction of atoms can occupy the first axial excited state. If we assume a 50% fraction, the coefficient α_3 is decreased by a factor 0.78, while α_2 is decreased by a factor 0.88. These systematic corrections are smaller than the statistical uncertainty in our data, so we neglect them in our initial analysis. We then can assume that the axial width is time independent.

In the first set of experiments, we have measured atom number as a function of time in the unitary regime at the Feshbach resonance (834 G), as shown in Fig. 1. The trap depth is set at 20% of the maximum attainable by reducing the laser intensity. The measured transverse energy of the cloud is $E_\perp/E_{F\perp} = 1.8$. We observe a significant ($> 60\%$) loss of the atoms in ~ 20 sec. The data is fit with Eq. 3. We find that a three-body decay curve fits the data very well while a two-body decay curve does not. This indicates that three-body inelastic collisions play a dominant role in the atom loss.

Fig. 2 shows the inelastic decay rate coefficient K_3 as a function of atomic density, at the Feshbach resonance, for $E_\perp/E_{F\perp} = 1.8$. The atomic density is varied by varying the final trap depth. Data are fit to three-body decay curves, from which we determine K_3. A constant value of K_3 over factor of 10 in atomic density indicates the atom loss is indeed a three-body decay process. By fitting all of the data with the same K_3, we obtain $K_3 = (8.44 \pm 1.04) \times 10^{-28}\mathrm{cm}^6/\mathrm{s}$.

We have also measured K_3 as a function of magnetic field for $\langle x^2\rangle/x_{F\perp}^2 = 1.8$, which corresponds to the transverse energy $E_\perp/E_{F\perp} = 1.8$ at resonance. The fitted K_3 is plotted as a function of interaction strength $1/k_{F\perp}a$, Fig. 3. Here $k_{F\perp} = (2mE_{F\perp})^{1/2}/\hbar$ is the two dimensional Fermi wave vector for an ideal gas at the trap center and a is the s-wave scattering length. By tuning the magnetic field from 790 G to 1200 G, we vary $1/k_{F\perp}a$ from 0.20 to -0.56, using the known values of $a(B)$ [22]. A factor of ~ 40 decrease in K_3 is observed as the bias magnetic field is tuned from the BEC regime to the BCS regime. We fit our data on the BCS side of the Feshbach resonance with the function of $K_3 = C|a|^n$ and find $n = 0.79 \pm 0.14$. The result is in significant disagreement with the theoretical prediction $n = 2.455$ [13]. On the BEC side, K_3 increases as the magnetic field is tuned away from the Feshbach resonance, instead of peaking on the resonance. This is consistent with the experiments by other groups [5, 6, 7].

We have repeated the measurement of atom number versus time, at resonance in the unitary regime, but at a lower energy $E_\perp/E_{F\perp} = 0.7$, Fig. 4. Neither two-body decay alone nor three-body decay alone fits the data. Instead, the combination of two-body and three-body decay fits the data well, which indicates two-body and three-body decays both contribute to the atom loss.

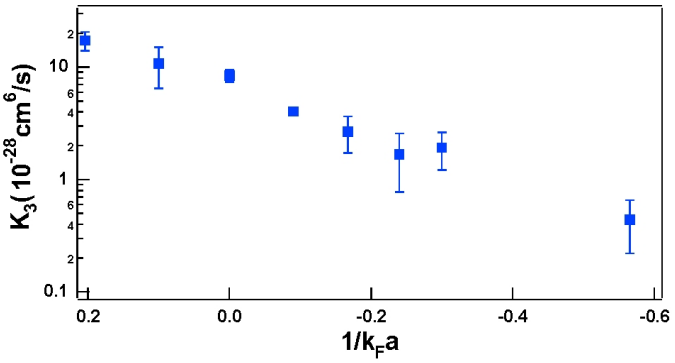

FIG. 3: K_3 versus interaction strength $1/k_{F\perp}a$ at $\langle x^2\rangle/x_{F\perp}^2 = 1.8$. Bars denote statistical error. Varying the magnetic field from 790 G to 1200 G changes $1/k_{F\perp}a$ from 0.20 to -0.56. We observe a factor of 40 change in K_3, from $(17.3 \pm 3.2) \times 10^{-28}\mathrm{cm}^6/\mathrm{s}$ at 790 G to $(0.44 \pm 0.22) \times 10^{-28}\mathrm{cm}^6/\mathrm{s}$ at 1200 G.

We suggest that the two-body process is related to correlated pairs that can exist at low energy (temperature). At higher energy, only single atoms exist while pairs are broken. In that case, the Fermi gas can only decay through three-body inelastic collisions of free atoms. By contrast, at low energy, pair-atom or pair-pair inelastic collisions are possible. Therefore, both two-body decay and three-body decay processes can play a role in the atom loss.

By measuring atom loss as a function of time at $E_\perp/E_{F\perp} = 0.7$, we find $K_3 = (3.30 \pm 1.81) \times 10^{-28}\mathrm{cm}^6/\mathrm{s}$ and $K_2 = (0.42 \pm 0.16) \times 10^{-14}\mathrm{cm}^3/\mathrm{s}$. It appears that K_3 is approximately three times smaller than that at $E_\perp/E_{F\perp} = 1.8$. This suppression cannot arise from Pauli blocking, as the energetic final states are unoccupied.

The observed scaling of K_3 with transverse energy is consistent with the prediction of Ref. [13], where $K_3 \propto E$ for the lowest order process. We observe $K_3(E_{F\perp} = 1.8)/K_3(E_{F\perp} = 0.7) = 8.44/3.30 = 2.56$, in very good agreement with the predicted ratio, $1.8/0.7 = 2.57$.

Although the data indicates a linear scaling of K_3 with energy, a decrease in K_3 can also arise from a reduction in the number of available single atoms, due to pair formation. Defining f as the fraction of atoms which are paired, the three-body decay rate is proportional to $(1-f)^3N^3$. For pair-atom collisions, a two-body rate would scale as $f(1-f)N^2$, while for pair-pair collisions, the corresponding rate would be proportional to f^2N^2.

Using these assumptions, we can rewrite the rate constants that appear in Eq. 3 as

$$\begin{aligned} K_3 &\equiv (1-f)^3 K_3^0 \\ K_2 &\equiv f\,K_2^0 \equiv f^2 K_{2,pp}^0 + f(1-f)K_{2,pa}^0. \end{aligned} \qquad (4)$$

Here $K_{2,pa}^0$ is the pair-atom inelastic collision rate coefficient and $K_{2,pp}^0$ is the pair-pair inelastic collision rate coefficient. At $E_\perp/E_{F\perp} = 1.8$, we observe pure three-

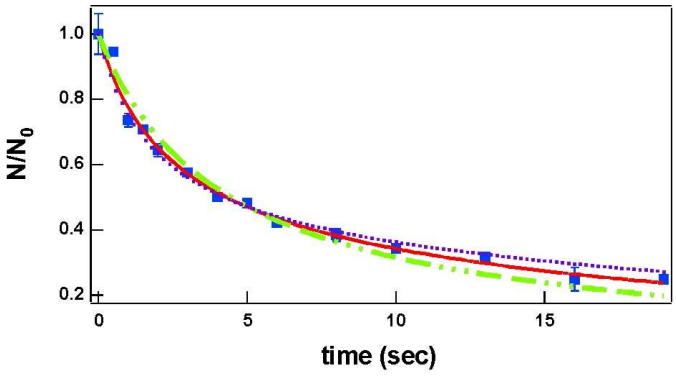

FIG. 4: Atom number versus time. Data were taken at $E_\perp/E_{F\perp} = 0.7$ in the unitary regime. Blue dots: Experimental data; Red solid curve: Combination fit including two-body and three-body decay; Violet dotted line: Three-body decay fit; Green dashed line: Two-body decay fit.

body decay so that $f = 0$. Hence we have $K_3^0 = K_3 = (8.44 \pm 1.04) \times 10^{-28}$ cm^6/s.

If we make the extreme assumption that K_3^0 is independent of energy, then we can reinterpret the fitted values of K_3 and K_2 for $E_\perp/E_{F\perp} = 0.7$ using Eq. 4 for the rate constants. $K_3 = (1-f)^3 K_3^0$ yields $f = (30 \pm 15)\%$ and $K_2 = fK_2^0$ then requires $K_2^0 = (1.72 \pm 1.04) \times 10^{-14}$cm^3/s. As the fraction of pairs appears large, it is more likely that the reduction in K_3 arises at least in part from energy scaling, which agrees with predictions [13], and that the true fraction of pairs is smaller.

At a magnetic field of 790 G, we first analyze the data to determine K_3 and K_2 of Eq. 3. For $\langle x^2\rangle/x_{F\perp}^2 = 1.8$, we find $K_3 = (17.3 \pm 3.2) \times 10^{-28}$cm^6/s. At $\langle x^2\rangle/x_{F\perp}^2 = 0.9$, we obtain, $K_3 = (9.35 \pm 3.06) \times 10^{-28}$cm^6/s, which is consistent with the predicted linear scaling with energy [13]. The corresponding two-body decay rate constants are $K_2 = 0$ at $\langle x^2\rangle/x_{F\perp}^2 = 1.8$ and $K_2 = (0.57 \pm 0.22) \times 10^{-14}$cm^3/s at $\langle x^2\rangle/x_{F\perp}^2 = 0.9$.

If we again assume instead that K_3^0 of Eq. 4 is independent of energy, we have $K_3^0 = (17.3 \pm 3.2) \times 10^{-28}$cm^6/s. Using $K_3 = (9.35 \pm 3.06) \times 10^{-28}$cm^6/s for $\langle x^2\rangle/x_{F\perp}^2 = 0.9$, we require the molecular fraction to be $f = (19 \pm 7)\%$. Then, we obtain $K_2^0 = (3.22 \pm 0.60) \times 10^{-14}$cm^3/s. Note that, on the BEC side, two-body inelastic collisions are expected to be molecule-atom or molecule-molecule, as predicted [16]. The increased two-body rate arising from molecules on the BEC side supports our assumption that the two-body rate at and just above resonance arises from correlated pairs. In this case, a many-body theory of inelastic collisions will be needed to replace the few-body theory that is valid far from resonance.

Above the Feshbach resonance, we do not observe a two-body decay process for $1/(k_{F\perp}a) \leq -0.09$, i.e., $B > 860$ G. This suggests that no pairs are formed for $B > 860$ G at the lowest energy $E_\perp/E_{F\perp} = 0.7$ we achieve.

By comparing the data at high energy and low energy over a wide range of density, we are able to distinguish between two-body and three-body processes. This method may provide a probe to determine the fraction of pairs or molecules in the Fermi gas, once the energy scaling of K_3 is fully established. In the unitary regime, investigation of the energy (or temperature [20]) dependence of K_3, as well as the pair fraction, will be an important topic of future work.

This research is supported by the Physics Divisions of the Army Research Office and the National Science Foundation, and the Chemical Sciences, Geosciences and Biosciences Division of the Office of Basic Energy Sciences, Office of Science, U.S. Department of Energy. We are indebted to Le Luo and Bason Clancy for help in the initial stages of this work.

* jet@phy.duke.edu

[1] E. Tiesinga, A. J. Moerdijk, B. J. Verhaar, and H. Stoof, Phys. Rev. A **46**, R1167 (1992).
[2] E. Tiesinga, B. J. Verhaar, and H. Stoof, Phys. Rev. A **47**, 4114 (1993).
[3] J. L. Roberts, N. R. Claussen, S. L. Cornish, and C. E. Wieman, Phys. Rev. Lett. **85**, 728 (2000).
[4] C. A. Regal, C. Ticknor, J. L. Bohn, and D. S. Jin, Phys. Rev. Lett. **90**, 053201 (2003).
[5] C. A. Regal, M. Greiner, and D. S. Jin, Phys. Rev. Lett. **92**, 083201 (2004).
[6] K. Dieckmann, C. A. Stan, S. Gupta, Z. Hadzibabic, C. H. Schunck, and W. Ketterle, Phys. Rev. Lett. **89**, 203201 (2002).
[7] T. Bourdel, L. Khaykovich, J. Cubizolles, J. Zhang, F. Chevy, M. Teichmann, L. Tarruell, S. J. J. M. F. Kokkelmans, and C. Salomon, Phys. Rev. Lett. **93**, 050401 (2004).
[8] K. M. O'Hara, S. L. Hemmer, M. E. Gehm, S. R. Granade, and J. E. Thomas, Science **298**, 2179 (2002).
[9] S. Giorgini, L. P. Pitaevskii, and S. Stringari, Rev. Mod. Phys. **80**, 1215 (2008).
[10] E. Braaten and H.-W. Hammer, Phys. Rept. **428**, 259 (2006).
[11] P. Bedaque, E. Braaten, and H.-W. Hammer, Phys. Rev. lett. **85**, 908 (2000).
[12] B. Esry, C. Greene, and J. Burke, Phys. Rev. lett. **83**, 1751 (1999).
[13] J. P. D'Incao and B. D. Esry, Phys. Rev. lett. **94**, 213201 (2005).
[14] E. Nielsen and J. Macek, Phys. Rev. lett. **83**, 1566 (1999).
[15] D. S. Petrov, Phys. Rev. A **67**, 010703(R) (2003).
[16] D. S. Petrov, C. Salomon, and G. V. Shlyapnikov, Phys. Rev. lett. **93**, 090404 (2004).
[17] P. Massignan and H. T. C. Stoof, Phys. Rev. A **78**, 030701(R) (2008).
[18] K. Helfrich and H.-W. Hammer (2009), arXiv:0902.3410.
[19] J. E. Thomas, Phys. Rev. A **78**, 013630 (2008).
[20] L. Luo and J. E. Thomas, J. Low Temp. Phys. **154**, 1 (2009).
[21] F. Werner, Phys. Rev. A **78**, 025601 (2008).
[22] M. Bartenstein, A. Altmeyer, S. Riedl, R. Geursen,

S. Jochim, C. Chin, J. H. Denschlag, and R. Grimm,
Phys. Rev. Lett. **94**, 103201 (2005).